

FTIR/PCA study of propanol in argon matrix: the initial stage of clustering and conformational transitions

Iryna Doroshenko¹, Vytautas Balevicius², George Pitsevich³, Kestutis Aidas²,
Valdas Sablinskas², and Valeriy Pogorelov¹

¹*Department of Experimental Physics, Taras Shevchenko National University of Kyiv
4 Glushkov Ave., Kyiv 03187, Ukraine*

²*Department of General Physics and Spectroscopy, Vilnius University
9-3 Sauletekio Al., Vilnius LT-10222, Lithuania
E-mail: dori11@ukr.net*

³*Department of Physical Optics, Belarusian State University, 4 Independence Ave., Minsk 220050, Belarus*

Received May 29, 2014, revised July 14, 2014
published online October 22, 2014

FTIR spectra of 1-propanol in an argon matrix were studied in the range 11 to 30 K. Principal component analysis of dynamic FTIR spectra and nonlinear band shape fitting has been carried out. The peaks of monomer, open dimer, mixed propanol-water dimer and those of higher H-bond clusters have been resolved and analyzed. The attribution of certain FTIR peaks has been supported by proper density functional theory calculations. Analyzing dependences of the integral band intensities of various aggregates on temperature it has been deduced that in the initial stage of clustering monomers and dimers are the basic building blocks forming higher H-bond clusters. The peaks assigned to two conformers of monomers and mixed propanol-water dimers were investigated processing the temperature dependences of their integral intensities in Arrhenius plot. The obtained values of $0.18 \text{ kJ}\cdot\text{mol}^{-1}$ for propanol monomer and $0.26 \text{ kJ}\cdot\text{mol}^{-1}$ for mixed dimer are well comparable with the energy differences between the global minimum conformation of 1-propanol (Gt) and some other energetically higher structures (Tt or Tg).

PACS: 36.40.Mr Spectroscopy and geometrical structure of clusters;
37.10.Pq Trapping of molecules;
78.30.-j Infrared and Raman spectra.

Keywords: FTIR spectra, propanol, argon matrix, clusters.

1. Introduction

Clusters, by definition, are aggregates of atoms/molecules with more or less regular and arbitrarily scalable repetition of basic building blocks. Their size is intermediate between atoms/molecule and the bulk. The growing interest to the clustering phenomena that produce partially ordered atomic or molecular structures is due to the recent developments and challenges in nanotechnologies, smart materials, heterogeneous systems, basic biochemical research, *etc.* [1,2] Convergence towards the bulk with increasing cluster size essentially depends on the nature of the observable physical properties, binding energies and on the resolution with which one looks at those. It is well-known that the hydrogen bond (H-bond) occupies in the scale of binding energies an intermediate place between

covalent and van der Waals interactions [3]. Therefore the simplest alcohols, molecules of which associate into various H-bond aggregates and even networks, can be considered as convenient models to investigate the cooperativity effects and the changes in the structural organization and conformations of molecular clusters sized over the nano- and mezzo-scales.

The most significant results on this field have been obtained using the vibrational spectroscopy (FTIR absorption and Raman) together with trapping/isolation in various cryogenic matrices [4–14]. This is mainly because the spectral acquisition carried out on isolated clusters at very low temperatures causes the appearance of narrow peaks with minimal band overlapping. Hence, it provides the possibility to study the spectral properties of individual clusters of different sizes and even various molecular conformers within

those clusters [4,5,8]. Thus the studies of small H-bond clusters of different size and conformations having the possibility to manipulate them and to resolve these effects in spectra experimentally can provide extremely valuable information for further progress in this field.

Note that in the most part of works on alcohols in matrices, droplets and jets the vibrational spectra were investigated at fixed temperatures. The variation of intensities of the bands of H-bonded and non-bonded alcohols was observed by changing the concentration of the investigated molecules, or by changing the matrix type, annealing, irradiation *etc.*, see e.g. Refs. 4, 5. The softening of the matrix by precisely increasing temperature and thus producing more wide paths (channels) to get alcohols molecules together can provide the effective tool to trace and to control the processes of molecular clustering continuously up to the bulk.

Continuing the studies on aggregation and relaxation processes of matrix-isolated alcohol molecules [7,13,14] the purpose of the present study was to analyze the FTIR spectra of 1-propanol molecules trapped in an argon matrix at continuously increasing temperature, *viz.*, stepping by 1 K, from $T = 11$ K to 30 K, *i.e.*, up to the onset of matrix evaporation that starts at 31 K. In order to improve the treatment of the experimental results the whole set of spectral data obtained under these conditions is processed applying the principal component analysis (PCA) with the sequent nonlinear curve fitting procedure. It is expected to obtain the novel set of data on the processes of molecular clustering and diffusion in a very initial stage as well as the conformational transitions at very low temperatures.

2. Experimental

Commercial 1-propanol was purified by standard methods [15]. The mixture of gaseous propanol and Ar (prepared by standard manometric techniques) in approximation

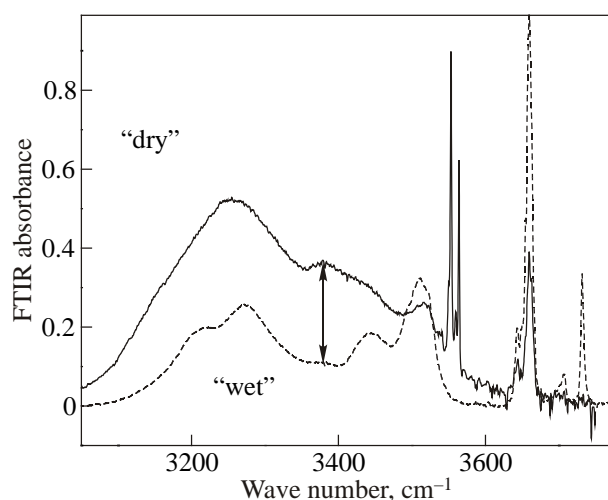


Fig. 1. Effect of drying of the sample using molecular sieves on FTIR spectra of 1-propanol in an argon matrix in O–H stretching region.

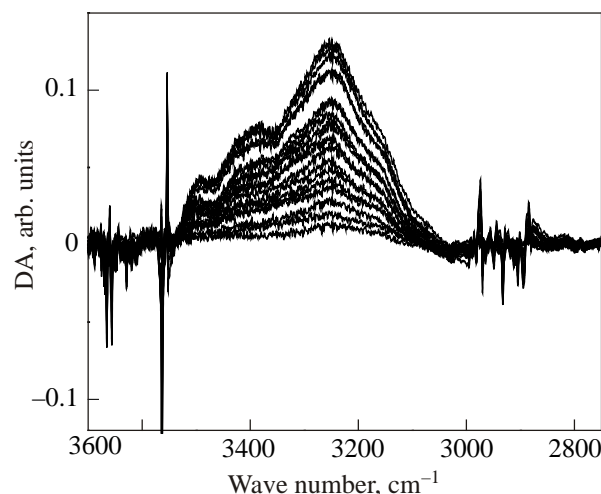


Fig. 2. Dynamic (difference) spectra obtained referring the measured 1D FTIR spectra to the “ground-state spectrum”, *i.e.*, to the spectrum at 11 K.

ratio 1:500 was deposited at 11 K and an average 4 mmol/h flow for 1 h onto CsI window. A particular attention was paid to the content of water in the sample. 1-propanol was dried using molecular sieves. The effect of drying on FTIR spectra was checked and shown in Fig. 1. Nevertheless some amount of water has still survived that caused the formation of mixed propanol-water dimers (see discussion below).

FTIR absorption spectra were measured at different temperatures from 11 K to 31 K by stepping $\Delta T = 1$ K using Bruker IFS 113 spectrometer equipped with liquid-N₂-cooled mercury cadmium telluride (MCT) detector at the resolution of 1 cm^{-1} in the $500\text{--}5000 \text{ cm}^{-1}$ region. In total 128 scans were averaged for each spectrum. Other details and the spectra are presented in Ref. 14.

An additional smoothing of the dynamic (difference) spectra (Fig. 2) during preprocessing procedures for PCA and nonlinear curve fitting was performed using the *Microcal Origin 9* and *Mathcad 15* packages [16,17].

3. DFT calculations

Geometry optimizations and harmonic vibrational frequency analysis of the considered molecular systems were performed at the density functional theory (DFT) level using a B3LYP functional [18] along with the 6-31++G** basis set [19]. We have considered only the so-called Gt conformer of 1-propanol which was found to be the lowest energy conformer at both DFT and coupled cluster levels [4,8,20]. We did not consider any vibrational frequency scaling. All computations were performed using Gaussian 09 program [21].

4. Results and discussion

In order to extract “hidden” information from complex spectra several powerful and versatile mathematical treatments of spectral data set have been developed. These

treatments are based e.g. on 2D correlation analysis (2DCOR) [22,23], moving windows 2D concept (MW2D) [24,25], factor (FA) and principal component analysis (PCA) [26–29], etc.

The main idea applying any of these methods is to analyze a set of spectral data acquired under the influence of an external perturbation [22,23]. An external perturbation can be any reasonable measure of a physical quantity, such as mechanical deformation, temperature or concentration. And indeed, some significant “composition-induced” changes in the FTIR spectra of 1-propanol in an Ar matrix are seen when the concentration increases from 1/300 to 1/150 [5]. However, it is obvious that the continuous perturbation of spectra using a “concentration” as the external variable is hardly to be precisely realized in the matrix isolation experiments. Therefore a “thermal” perturbation has been chosen for the present study as more preferable.

In the present work in order to improve the earlier applied 2DCOR analysis of the conventional experimental FTIR spectra of 1-propanol in an Ar matrix [14] the dynamic spectra were obtained and the whole set of data was processed applying the PCA with the sequent nonlinear curve fitting procedure.

The dynamic (difference) spectra $DA(\omega, T)$ have been obtained from the conventional FTIR spectra (1D spectra) [14] referring those to the “ground-state spectrum”, i.e., to the spectrum at the lowest temperature (11 K). The dynamic spectra are shown in Fig. 2. In the present work the temperature behavior of the integral intensities of the $\nu\text{C-H}$ bands ($2800\text{--}3000\text{ cm}^{-1}$) was checked in addition. These intensities remain practically unchanged over the whole temperature range and thus indicate that the evaporation of 1-propanol at the heating within 11–30 K is negligible. It means that no additional renormalization of intensities in the processing of dynamic spectra was necessary. However several negative peaks appearing in the dynamic spectra at $3660, 3643, 3564, 3553\text{ cm}^{-1}$ that correspond to $\nu\text{O-H}$ band group of monomer and most probably mixed dimer and also at some parts of $\nu\text{C-H}$ band group. These negatives peaks are caused by the decrease of monomeric and dimeric species with increasing temperature (see discussion below) and by the conformational transitions of 1-propanol molecules [4].

The processing of experimental data using PCA was realized in the following steps. The original spectra were baseline corrected and slightly smoothed using the “ksmooth” function, which applies a Gaussian kernel to create weighted averages of the absorption values. This procedure is implemented in Mathcad code [21]. The data matrix \mathbf{D} was composed by placing the dynamic spectra $DA(\omega_i, T_j)$, $i = 1\dots n, j = 1\dots m$ into m rows. The corresponding covariance matrix was then obtained multiplying \mathbf{D} by its transpose \mathbf{D}^T :

$$\mathbf{Z} = \mathbf{D} \cdot \mathbf{D}^T. \tag{1}$$

This way of construction of \mathbf{Z} is called the sample-sample (SS) approach [28]. It differs from the variable-variable (VV) approach ($\mathbf{Z} = \mathbf{D}^T \cdot \mathbf{D}$), which is traditionally used in 2DCOR [14,22,23] or when 2DCOR and PCA are applied in tandem [29,30].

The dimension of the covariance matrix \mathbf{Z} in the SS approach is $m \times m$ whereas it would be $n \times n$ if the VV approach applied. The values of m (the number of spectra registered at different external perturbations) and n (the number of points in the spectrum) usually vary $m \sim 10\text{--}10^2, n \sim 10^2\text{--}10^3$. Thus the data processing in the SS approach, i.e., working with \mathbf{Z} matrix of order of only hundreds elements, allows saving the computing resources very significantly, particularly in the next steps of the treatment where the loads vectors (\mathbf{p}_j) are obtained by solving

$$\mathbf{Z} \cdot \mathbf{p}_j = \lambda_j \cdot \mathbf{p}_j, \tag{2}$$

where λ_j is the eigenvalue associated with the eigenvector \mathbf{p}_j [31]. The scores vectors (\mathbf{t}_j) were then calculated as

$$\mathbf{t}_j = \mathbf{D}^T \cdot \mathbf{p}_j. \tag{3}$$

The overlapped spectral components are clearly resolved on the scores vectors for the first three principal components $t_j, j = 1\text{--}3$ (Fig. 3). The number of the statistically significant PCs was evaluated using the factor indicator function, which reaches a minimum when the correct number of factors (components) is employed [26,32]. It was found that statistically significant can be first five PCs. However, the scores for the fourth and fifth PCs looked like a noise and therefore were not analyzed. The main peaks resolved in \mathbf{t}_j are shown by block arrows in Fig. 3. These maximum positions were further used as the zero-order approach input data in the nonlinear curve fitting of experimental FTIR spectra by a set of Lorentz functions.

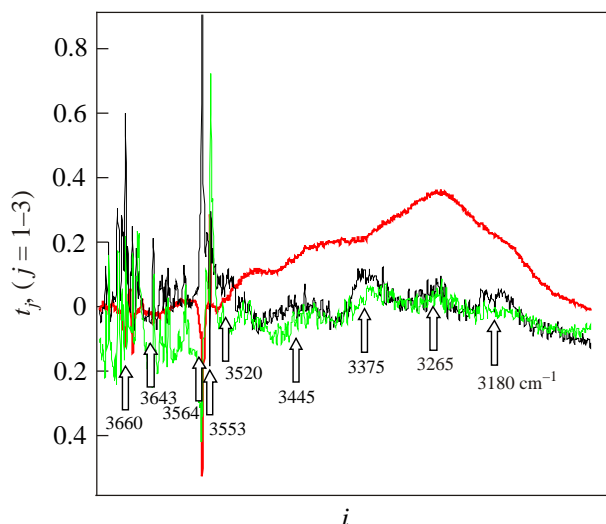


Fig. 3. (Color online) PCA processing of the dynamic FTIR spectra of 1-propanol in Ar matrix in the temperature range of 12–30 K: scores vectors for the first ($\lambda_1 = 91.006$), second ($\lambda_2 = 0.293$) and third ($\lambda_3 = 0.095$) PC.

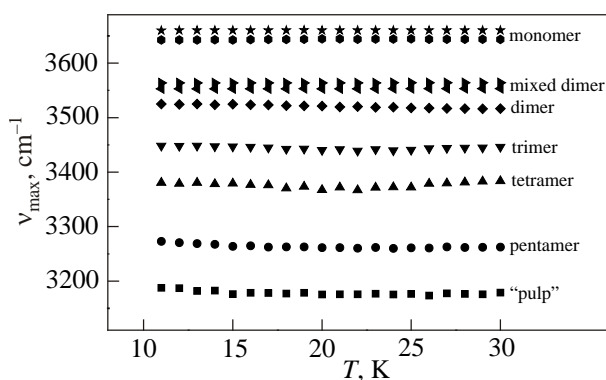


Fig. 4. Maximum positions of resolved O–H stretching bands obtained using nonlinear band shape fitting of experimental FTIR spectra by a set of Lorentz functions.

The revised values of maximum position in the whole studied temperature range are presented in Fig. 4.

The general trend in the assignment of the H-bond bands ($3000\text{--}3600\text{ cm}^{-1}$) in simple alcohols, most frequently met in the literature, looks like — “the lower band frequency the higher aggregate”. In many cases this is confirmed by proper quantum chemistry calculations [4,5,8,12]. Following this scheme, the sharp peaks of the highest frequencies, i.e., at 3660 and 3643 cm^{-1} (Figs. 2–4), were assigned to the O–H stretching vibration of monomer conformers. The band at 3521 cm^{-1} can be definitely attributed to an open dimer of 1-propanol [4,5,8].

A trickier situation is with the peaks at 3564 and 3553 cm^{-1} . These bands are absent in many other works on 1-propanol studies [4,5,8]. We like to suppose that they might be originated from the conformers of mixed propanol-water dimers. Such structures can get into the matrix due to not enough proper drying technique or other experimental setup applied in the present work. However, these peaks, being narrow and well resolved, can be also used studying the conformational behavior of 1-propanol.

In order to check this assumption geometry optimizations and analysis of harmonic vibrational frequencies and intensities of the considered molecular systems were performed at the level of theory given above. The results are presented in Fig. 5. It comes out that the peak between those of monomer and open dimer (Fig. 5(c)) indeed can be interpreted as the band of the mixed propanol-water dimer with propanol as the hydrogen bond donor. In the case of the mixed dimer with water as H-bond donor the band of O–H stretching would appear at lower wave numbers than in the open dimer (Figs. 5(b), (d)).

The remaining bands between $3448\text{--}3264\text{ cm}^{-1}$ (Fig. 4) should be attributed to the higher 1-propanol clusters from trimer to pentamer. Finally, the extremely broad feature at ca 3178 cm^{-1} can be assigned as a “pulp” — i.e., highly disordered H-bond manifolds/polymers [5,14].

The intensities of all H-bond bands, except those of monomer and dimer, increase with temperature. No negative

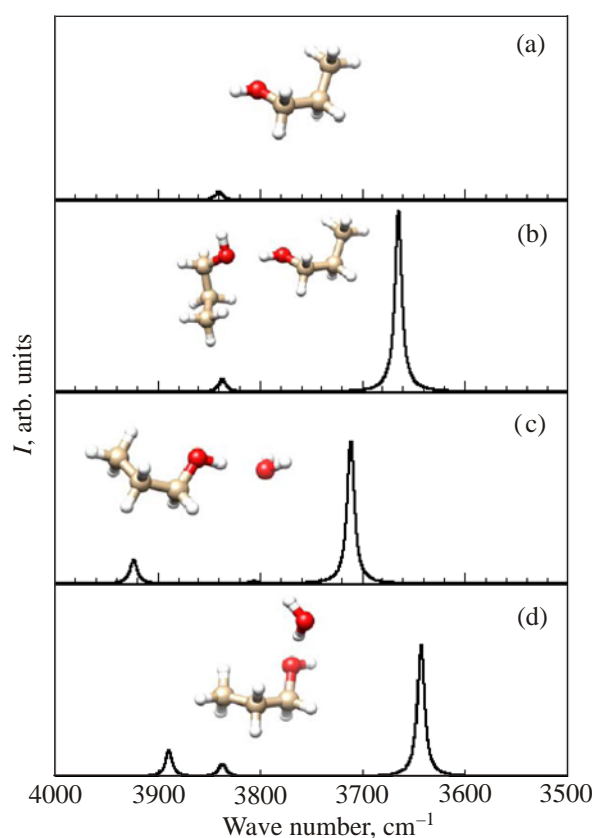


Fig. 5. Calculated vibrational spectra of 1-propanol in O–H stretching region for monomer (a), open dimer (b), mixed propanol — water dimers with propanol as donor (c) and acceptor (d), respectively.

DA peaks are seen in the dynamic spectra in the spectral range of higher H-bond aggregates (Fig. 2). This means that monomers and dimers are in the initial clustering stage the main “building bricks”, and their diffusion sustains

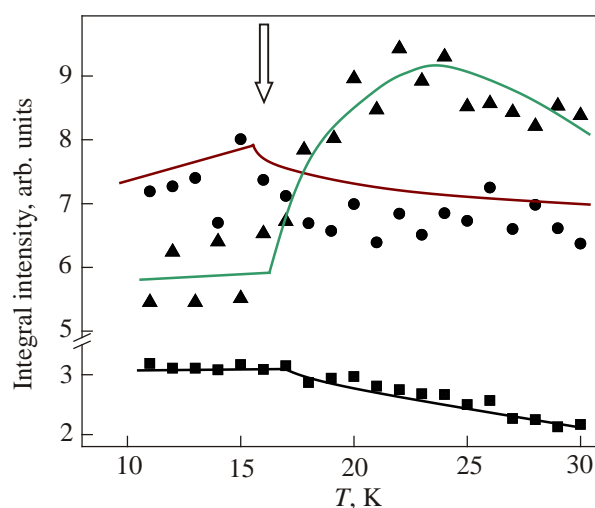


Fig. 6. Temperature dependences of integral intensities of monomer: 3660 cm^{-1} (■), open dimer 3521 cm^{-1} (●) and trimer 3444 cm^{-1} (▲) bands. The onset of intensive monomer and dimer diffusion in the matrix is shown by block arrow.

the formation of higher H-bond aggregates. This is rather clearly pronounced on the dependencies of integral intensities of monomer and dimer bands on temperature (Fig. 6). More intensive diffusion of monomers and dimers starts

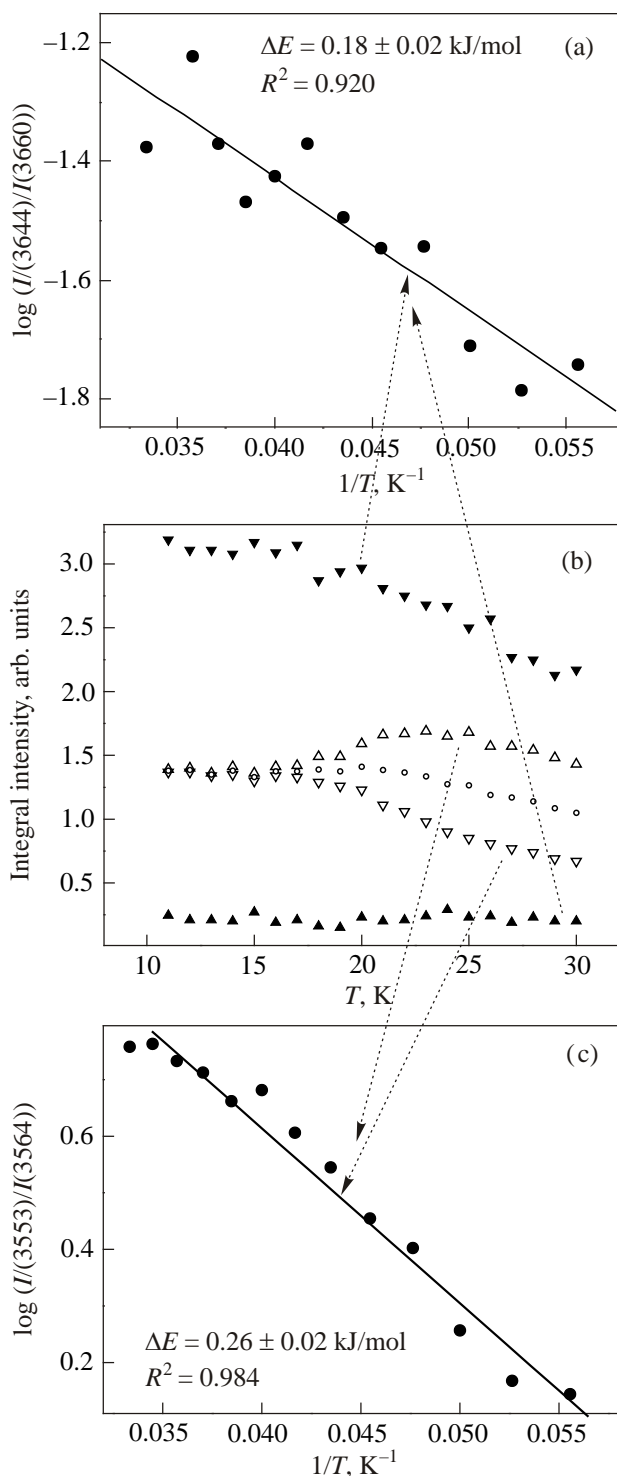


Fig. 7. Temperature dependences of the integral intensities of monomer: 3660 cm^{-1} (\blacktriangledown), 3644 cm^{-1} (\blacktriangle), open dimer bands: 3553 cm^{-1} (\triangle), 3564 cm^{-1} (∇), the average value $(I(3553) + I(3564))/2$ (\bullet) (b); Arrhenius plots to estimate the energy differences between conformations (a) and (c).

at $\sim 17\text{ K}$. This can be due to the matrix softening by increasing temperature, and thus the opening of wider channels for molecular diffusion, leading to the increasing discharge of “monomeric” (A_1) and “dimeric” (A_2) states by elementary binding reactions $A_1 + A_{n-1} \rightarrow A_n$ and $A_2 + A_{n-2} \rightarrow A_n$. The irreversibility of kinetic processes in the matrices does not let to refill these states (A_1 and A_2) by thermal chemical equilibrium, as it is common for gases and liquid solutions. Note that at ca 24 K the Ar matrix becomes spongy enough that the dynamics of higher H-bond aggregates, viz. trimers, would be enhanced also — the integral intensity of trimer band starts to decrease at this temperature (Fig. 6).

The energetic picture of 1-propanol conformers and conformational transitions in the gas phase, jets and matrices have been studied experimentally using FTIR, Raman and Microwave (MW) spectroscopy techniques as well as using high level calculations (see Refs. 4 and 8 and the references cited therein). The authors noted that some experimental energy differences between different conformations of 1-propanol can be smaller than those predicted by high level quantum calculations. Nevertheless the Gt conformation was found to be the global minimum structure at all used levels of theory (the nomenclature of conformers used is the same as in Ref. 8).

The sharp peaks at 3660 and 3644 cm^{-1} as well as those at 3564 and 3553 cm^{-1} , observed in the present work and assigned to the conformers of 1-propanol monomer and mixed dimer with water, respectively, were investigated more thoroughly. The dependences of their integral intensities on temperature were converted and processed in Arrhenius plot (Fig. 7). The obtained values of $0.18\text{ kJ}\cdot\text{mol}^{-1}$ for propanol monomer and $0.26\text{ kJ}\cdot\text{mol}^{-1}$ for mixed dimer are well comparable with the energy differences between the global minimum conformation of 1-propanol (Gt) and some other energetically higher structures (Tt or Tg) evaluated by recent high level quantum chemical calculations [4,8,20,33]. However, energy differences that are below $\sim 1\text{ kJ}\cdot\text{mol}^{-1}$ are challenging to theories. Therefore for more rigorous conclusions the wave number differences of O–H stretching bands between local minima and the global minimum conformation should be compared in addition to the energy arguments. The experimentally observed wave-number differences of -16 cm^{-1} (monomer peaks) and -11 cm^{-1} (mixed dimer peaks) point to the Gt-Tg conformational transition since in the case of Gt-Tt transition much less values (-2 to -5 cm^{-1}) are expected [8].

Conclusions

The dynamic FTIR spectra of 1-propanol in an argon matrix have been studied using temperature as an external perturbation from $T = 11\text{ K}$ to 30 K stepping by 1 K . The principal component analysis (PCA) has been carried out, the main attention concentrating to 1-propanol O–H stretch-

ing vibrations at 3000–3700 cm^{-1} . The peaks of monomer, open dimer, mixed propanol-water dimer as well as the H-bond clusters from trimer to pentamer have been resolved in the spectra.

Analyzing the dependences of the integral band intensities for various clusters on temperature it has been deduced that in the initial clustering stage monomers and dimers are the basic building blocks, the diffusion of which above *ca* 17 K sustains the formation of higher H-bond structures. At *ca* 24 K the Ar matrix becomes spongy enough that the diffusion of higher H-bond aggregates, viz. trimers, also would be enhanced.

The peaks assigned to two conformers of monomer and mixed propanol-water dimers with propanol as H-bond donor were investigated by processing their temperature dependences of integral intensities in Arrhenius plot. The obtained values of 0.18 $\text{kJ}\cdot\text{mol}^{-1}$ for monomer and 0.26 $\text{kJ}\cdot\text{mol}^{-1}$ for mixed dimer are well comparable with the energy differences between the global minimum conformation (Gt) and some other energetically higher conformers (most probably Tg).

Acknowledgments

Funding from the European Community's social foundation under Grant Agreement No VP1-3.1-ŠMM-08-K-01-004/KS-120000-1756, the State Fund for Fundamental Researches of Ukraine (grant No F54.1/008) and the State Foundation for Basic Research of Belarusian Republic (grant No F13K - 064) are acknowledged. The authors thank the High Performance Computing Center "HPC Sauletekis" of Faculty of Physics at Vilnius University for computational resources. Professors Martin Suhm, Stephane Coussan and Jozse Grdadolnik are thanked for the comments and stimulating discussions.

1. P.G. Reinhard and E. Suraud, *Introduction to Cluster Dynamics*, Wiley-VCH, Weinheim (2004).
2. G. Schmid, *Nanoparticles: from Theory to Application*, Wiley-VCH, Weinheim (2004).
3. E. Arunan, G.R. Desiraju, R.A. Klein, J. Sadlej, S. Scheiner, I. Alkorta, D.C. Clary, R.H. Crabtree, J.J. Dannenberg, P. Hobza, H.G. Kjaergaard, A.C. Legon, B. Mennucci, and D.J. Nesbitt, *Pure Appl. Chem.* **83**, 1619 (2011).
4. T.N. Wassermann, M.A. Suhm, P. Roubin, and S. Coussan, *J. Mol. Struct.* **1025**, 20 (2012).
5. N. Michniewicz, A.S. Muszynski, W. Wrzeszcz, M.A. Czarnecki, B. Golec, J.P. Hawranek, and Z. Mielke, *J. Mol. Struct.* **887**, 180 (2008).
6. Z. Mielke, S. Coussan, K. Mierzwicki, P. Roubin, and M. Saldyka, *J. Phys. Chem. A* **110**, 4712 (2006).
7. G. Pitsevich, I. Doroshenko, V. Pogorelov, V. Sablinskas, and V. Balevicius, *Fiz. Nizk.* **39**, 499 (2013) [*Low Temp. Phys.* **39**, 389 (2013)].
8. T.N. Wassermann, P. Zielke, J.J. Lee, C. Cezard, and M.A. Suhm, *J. Phys. Chem. A* **111**, 7437 (2007).
9. C. Emmeluth, P. Dyczmons, and M.A. Suhm, *J. Phys. Chem. A* **110**, 2906 (2006).
10. R.A. Provencal, J.B. Paul, K. Roth, C. Chapo, R.N. Casaes, R.J. Saykally, G.S. Tschumper, and H.F. Schaefer III, *J. Chem. Phys.* **110**, 4258 (1999).
11. S. Coussan, V. Brenner, J.P. Perchard, and W.Q. Zheng, *J. Chem. Phys.* **113**, 8059 (2000).
12. S. Coussan, Y. Bouteiller, A. Loutellier, J.P. Perchard, S. Racine, A. Peremans, W.Q. Zheng, and A. Tadjeddine, *Chem. Phys.* **219**, 221 (1997).
13. V. Pogorelov, I. Doroshenko, P. Uvdal, V. Balevicius, and V. Sablinskas, *Mol. Phys.* **108**, 2165 (2010).
14. V. Balevicius, V. Sablinskas, I. Doroshenko, and V. Pogorelov, *Ukr. J. Phys.* **56**, 855 (2011).
15. B.S. Furniss, A.J. Hannaford, P.W.G. Smith, and A.R. Tatchell, *Vogel's Textbook of Practical Organic Chemistry*, Pearson Education Ltd, Singapore (1989).
16. OriginLab Corporation, <http://www.OriginLab.com>.
17. <http://www.ptc.com/product/mathcad/>.
18. A.D. Becke, *J. Chem. Phys.* **98**, 5648 (1993).
19. W.J. Hehre, R. Ditchfield, and J.A. Pople, *J. Chem. Phys.* **56**, 2257 (1972).
20. S. Höfener, F.A. Bischoff, A. Glöß, and W. Klopper, *Phys. Chem. Chem. Phys.* **10**, 3390 (2008).
21. M.J. Frisch, G.W. Trucks, H.B. Schlegel, G.E. Scuseria, M.A. Robb, J.R. Cheeseman, G. Scalmani, V. Barone, B. Mennucci, G.A. Petersson, H. Nakatsuji, M. Caricato, X. Li, H.P. Hratchian, A.F. Izmaylov, J. Bloino, G. Zheng, J.L. Sonnenberg, M. Hada, M. Ehara, K. Toyota, R. Fukuda, J. Hasegawa, M. Ishida, T. Nakajima, Y. Honda, O. Kitao, H. Nakai, T. Vreven, J.A. Montgomery, Jr., J.E. Peralta, F. Ogliaro, M. Bearpark, J.J. Heyd, E. Brothers, K.N. Kudin, V.N. Staroverov, T. Keith, R. Kobayashi, J. Normand, K. Raghavachari, A. Rendell, J.C. Burant, S.S. Iyengar, J. Tomasi, M. Cossi, N. Rega, J.M. Millam, M. Klene, J.E. Knox, J.B. Cross, V. Bakken, C. Adamo, J. Jaramillo, R. Gomperts, R.E. Stratmann, O. Yazyev, A.J. Austin, R. Cammi, C. Pomelli, J.W. Ochterski, R.L. Martin, K. Morokuma, V.G. Zakrzewski, G.A. Voth, P. Salvador, J.J. Dannenberg, S. Dapprich, A.D. Daniels, O. Farkas, J.B. Foresman, J.V. Ortiz, J. Cioslowski, and D.J. Fox, *Gaussian 09, Revision D.001, Inc.*, Wallingford CT, 2013.
22. I. Noda and Y. Ozaki, *Two-Dimensional Correlation Spectroscopy — Applications in Vibrational and Optical Spectroscopy*, Wiley, Chichester (2004).
23. I. Noda, *Vib. Spectrosc.* **60**, 146 (2012).
24. M. Thomas and H.H. Richardson, *Vib. Spectrosc.* **24**, 137 (2000).
25. S. Morita, H. Shinzawa, R. Tsenkova, I. Noda, and Y. Ozaki, *J. Mol. Struct.* **799**, 111 (2006).
26. E.R. Malinowski, *Anal. Chem.* **49**, 606 (1977).
27. B.G.M. Vanderginste, D.L. Massart, L.M.C. Buydens, S. De Jong, P.J. Lewi, and J. Smeyers-Verbeke, *Handbook of*

- Chemometrics and Qualimetrics*, Elsevier Science B.V., Amsterdam, The Netherlands (1998), Part B.
28. V.H. Segtnan, S. Sasic, T. Isaksson, and Y. Ozaki, *Anal. Chem.* **73**, 3153 (2001).
 29. B. Czarnik-Matuszewitz, S.B. Kim, Y.M. Jung, *J. Phys. Chem. B* **113**, 559 (2009).
 30. V. Aleksa, J. Kausteklis, V. Klimavicius, Z. Gdaniec, and V. Balevicius, *J. Mol. Struct.* **993**, 91 (2011).
 31. C. Thibault, P. Huguet, P. Sizat, and G. Pourcelly, *Desalination* **149**, 429 (2002).
 32. V. Balevicius and H. Fuess, *Chem. Phys. Lett.* **377**, 530 (2003).
 33. K. Kahn and T.C. Bruice, *Chem. Phys. Chem.* **6**, 487 (2005).
 34. A. Maeda, F.C. De Lucia, E. Herbst, J.C. Pearson, J. Riccobono, E. Trosell, and R.K. Bohn, *Astrophys. J., Suppl. Ser.* **162**, 428 (2006).